# Stabilization of transverse solitary waves by a nonlocal response of the nonlinear medium

Dieter Suter and Tilo Blasberg
*Institute of Quantum Electronics, Swiss Federal Institute of Technology–Zürich, CH-8093 Zürich, Switzerland*
(Received 23 July 1993)

Optical pumping of atomic vapors can lead to self-focusing of resonant laser beams. The saturation of the optical pumping process at low intensity allows the study of transverse solitons in the form of self-trapped laser beams, using low-power cw lasers. The long lifetime of the optically pumped atoms allows the atomic diffusion to transport the excitation away from the interaction region. Numerical simulations show that the resulting nonlocal response of the medium represents an important mechanism that stabilizes the self-trapped beam. The theoretical predictions are confirmed by experimental results from sodium vapor.

PACS number(s): 42.65.Jx, 42.50.Rh

Self-focusing of laser beams in nonlinear optical media [1–3] is one of the best examples of spontaneous formation of (spatially) localized structures due to nonlinear processes. Self-focusing occurs if the total index of refraction increases with the laser intensity, as in many Kerr media. Laser beams with Gaussian intensity profiles then induce a refractive index profile, which has the same effect as a convex lens, thereby counteracting the normal effect of diffraction. When the two effects cancel each other, the beam can propagate without diffraction; it is then said to be self-trapped [4,5]. Since both the Kerr effect leading to self-focusing and the opposing tendency of light to diffract are indirectly proportional to the cross-sectional area of the beam, the self-trapped state is unstable in ideal three-dimensional Kerr media [3,6]. If the laser intensity is below a critical intensity that depends on the nonlinearity of the medium, the beam diffracts as usual. Above the critical intensity, the beam self-focuses to an area of the dimension of the optical wavelength [7], unless damage to the material stops the process [2]. At the critical intensity, the beam can propagate without diffracting, but arbitrarily small perturbations cause it to fall into either of the two other regimes. In two-dimensional systems, such as planar waveguides, self-trapped beams can be stable and lead to nondiffracting beams [8–10]. In analogy to other stable, localized solutions of nonlinear wave equations, such self-trapped beams have been called "spatial solitary waves" or "transverse solitons."

While Derrick's theorem [6] precludes the existence of stable, time-independent solutions of nonlinear wave equations that are localized in more than one spatial dimension, it is well known [3] that laser beams can be self-trapped in three-dimensional media, when the index of refraction does not increase indefinitely with intensity, but saturates before the material suffers laser-induced damage. In such a medium, the laser beams can become localized in the two transverse dimensions. In general, its diameter is not time independent, but shows characteristic oscillations that reflect the competing effects of self-focusing and diffraction [3,11,12]. This saturation effect had already been proposed as the relevant mechanism for the formation of the small-scale filaments that tend to form in many self-focusing processes after the collapse of the beam [13]. For the implementation of such a scheme, resonant atomic media offer several advantages: due to the resonant enhancement of the interaction, nonlinear effects appear at low intensities. Also, the nonlinear refractive-index change can easily be saturated, even with a low-power ($\leq 100$ mW) cw laser. In addition, the nonlinear optical properties are of the same order of magnitude as the linear effect and both the linear and nonlinear contributions can be adjusted by tuning the laser frequency close to an optical transition frequency. Atomic vapors, in particular, have the additional advantage of being essentially immune to damage and allow large variations of the refractive index by changing the particle density through the temperature.

Early demonstrations of this type of experiment were reported by Grischkowsky [14] and by Bjorkholm and Ashkin [5], who used cw lasers to achieve not only self-focusing, but also self-trapping. Subsequent work by other groups improved the understanding of these experiments by treating the atomic medium as an ensemble of two-level atoms [15–18]. Yabuzaki, Hori, and Kitano [19] suggested that optical pumping with circularly polarized light should cause self-focusing at even lower power. We have implemented this scheme for the generation of transverse solitary waves in a three-dimensional medium. In our setup, atomic sodium serves as the nonlinear medium. A circularly polarized laser beam, tuned close to the $D_1$ transition, optically pumps the Na atoms. If the laser frequency is blue detuned, where the index of refraction is less than unity, the optical pumping increases the total index of refraction at the center of the beam, as required for self-focusing. However, since the optical pumping process cannot increase the index of refraction above unity, the nonlinearity saturates and the self-trapped state is stabilized.

For a theoretical description of this process, we start from the usual nonlinear wave equation in the paraxial wave approximation

$$k\frac{\partial}{\partial z}A^2 = -\nabla_\perp\cdot(A^2\nabla_\perp\phi)\ , \tag{1}$$

 

$$\frac{\partial}{\partial z}\phi=-\frac{1}{2k}(\nabla_\perp\phi)^2+\frac{k}{2}\left[\frac{\nabla_\perp^2 A}{k^2 A}+2\frac{\Delta n}{n_0}\right], \tag{2}$$

where $Ae^{i\phi}$ represents the slowly varying complex field amplitude, $k$ the wave vector, $n_0$ the linear refractive index, and $\nabla_\perp$ refers to the transverse coordinates $r,\theta$. In a homogeneous system, optical pumping changes the refractive index $n=n_0+\Delta n$ by

$$\Delta n=(1-n_0)\alpha A^2/(\alpha A^2+\gamma_0), \tag{3}$$

where $\alpha A^2$ represents the optical pumping rate and $\gamma_0$ the rate at which the atomic polarization decays [20–22]. The induced index change $\Delta n$ is therefore in the range $0\le\Delta n\le 1-n_0$. If the laser is blue detuned from an optical resonance frequency, the linear refractive index $n_0$ is smaller than unity, $n_0<1$, and $\Delta n$ is positive. The phase velocity is therefore smallest in the center of the beam and self-focusing is possible. In addition, the refractive index cannot exceed unity, since $\Delta n$ saturates for high enough intensity, $\alpha A^2\gg\gamma_0$.

In the actual experiment, we also have to take the effect of atomic motion into account. If the mean-free path of the atoms is small compared to the diameter of the laser beam, we can describe the motion as a diffusion process. The refractive index change is then determined by the equation

$$\frac{\partial}{\partial t}\Delta n(r,t)=\alpha A^2[1-n_0-\Delta n(r,t)]-\gamma_0\Delta n(r,t)+D\left[\frac{\partial}{\partial r^2}+\frac{1}{r}\frac{\partial}{\partial r}\right]\Delta n(r,t), \tag{4}$$

where $D$ represents the diffusion constant. Through the diffusion term, the index depends now not only on the local field amplitude, but also on a spatially averaged intensity.

Figure 1 illustrates this effect: Figure 1(a) shows the connection between the laser intensity and the refractive index for the case of a local response of the medium: the nonlinear index change extends over the same spatial region as the laser beam. Figure 1(b) shows the contrasting effect due to atomic diffusion: in this case, the index change extends well beyond the laser-beam diameter. The effect of diffusion on the resulting index profile can be shown most directly by making the following assumptions: (1) the laser beam has a cylindrical intensity profile with radius $r_0$ and propagates along the axis of a cylindrical cell of radius $R$. (2) The relaxation vanishes inside the sample volume, but is instant on the surface of the sample cell, i.e., $\gamma_0=0$, $\Delta n(R,t)=0$. (3) The optical pump rate is sufficiently large that the index change $\Delta n$ within the laser beam reaches the maximum possible value $\Delta n_{\max}=1-n_0$. In this case, the resulting index profile has a logarithmic dependence on the distance from the laser beam,

$$\Delta n(r)=\Delta n_{\max}\frac{\ln(r/R)}{\ln(r_0/R)}. \tag{5}$$

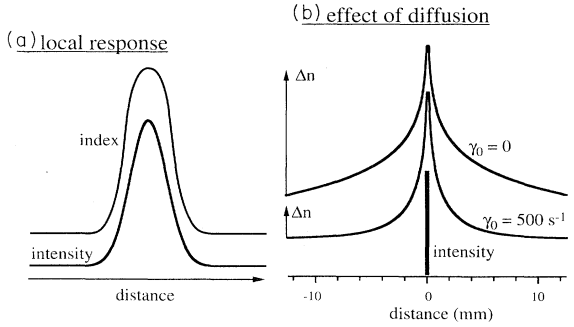


FIG. 1. Local (a) and nonlocal (b) response of an optically nonlinear medium. The left-hand part shows schematically the case of a solid or an atomic gas with a short lifetime of the nonlinearity; the right-hand part shows the effect of diffusion for two different relaxation rates.

These assumptions are sufficiently close to actual experimental conditions that the index profile is a good approximation to an experimental one.

A nonvanishing relaxation rate $\gamma_0$ reduces the effect of diffusion. The second curve in Fig. 1(b) illustrates this for a relaxation rate $\gamma_0=500\ \text{sec}^{-1}$; the resulting index profile has become visibly narrower compared to the case without diffusion. Note that the origin of the $y$ axes is not the same for the three curves in this part of the figure. Both index profiles reach zero at the walls of the sample cell [23] and the same maximum at the center. The physical mechanism causing these relaxation processes can include collisions with buffer-gas atoms [24]. However, under typical experimental conditions used for self-focusing experiments, other effects are considerably more effective. In particular, the high number densities required for effective self-focusing lead to significant radiation-trapping effects, which contribute to the relaxation rate [23,25].

The effect of diffusion depends therefore on the relative size of the diffusion rate $D$ and the relaxation rate $\gamma_0$. A good estimate of the cross-sectional area $A$ of the induced waveguide is $A=D/\gamma_0$. For the example shown in Fig. 1, we used the experimentally determined value for the diffusion constant $D=5\times10^{-3}\ \text{m}^2\text{sec}^{-1}$, and a relaxation rate $\gamma_0=500\ \text{sec}^{-1}$. With these values, the above estimate yields an effective cross section $A=0.1\ \text{cm}^2$, corresponding to a radius of 1.8 mm, in good agreement with the calculated profile. The radius of the induced waveguide can therefore become much larger than the radius of the laser beam, which was set to 0.1 mm in the calculation. Since this effect depends on the relaxation rate $\gamma_0$, it is effective only for optical nonlinearities due to ground-state polarization. If the optical nonlinearity is due to saturation of an optical transition [14,5], the decay rate $\gamma_0$ of the refractive index profile is the relaxation rate of the excited-state population. For a strong optical transition, the range of the medium response is then limited to a few micrometers, some three orders of magnitude less than in the case considered here.

To show the effects of this nonlocal response on the self-trapping dynamics, we have numerically integrated the equations of motion (1), (2), and (4), using the following parameters: $k=10.66\ \mu\text{m}^{-1}$ (Na $D_1$ transition),

$n_0 = 1-7\times10^{-5}$, and the incident laser-beam amplitude was a plane wave with Gaussian cross section and a beam diameter of 36 $\mu$m [full width at half-maximum (FWHM)]. The maximum pump rate was chosen as $\alpha A_{\max} = 3\times10^7$ sec$^{-1}$, corresponding to an intensity of 2 kW cm$^{-2}$ at a normalized laser detuning of $\bar{\Delta}=5$ [22], or a laser-beam power of 26 mW. The relaxation rate $\gamma_0$ was set to the experimentally observed value of $10^4$ sec$^{-1}$, corresponding to a diffusion-induced width of the waveguide of $\sqrt{D/\gamma_0}=400$ $\mu$m, an order of magnitude larger than the laser-beam diameter. In Fig. 2, we show the effect on the self-focusing process: the absolute value of the laser amplitude is plotted as a function of the distance from the center of the laser beam. Successive traces correspond to cross sections farther into the medium. The data in Fig. 2(a) illustrate the case of purely local response of the system, corresponding to a vanishing diffusion constant. In this case, the initially Gaussian shape of the laser beam is apparently unstable; it separates into a ring structure whose diameter increases as the beam propagates farther into the medium. Similar structures are well known from self-focusing experiments in dielectric solids [3]. The data shown in Fig. 2(b) were calculated with identical parameters, except that the diffusion coefficient was now set to the experimentally determined value of $D=5000$ $\mu$m$^2$/$\mu$sec. In this case, the laser beam remains stable, apart from a small amplitude oscillatory motion of the beam shape. This qualitatively different behavior is apparently due to the nonlocal response of the atomic medium, which stabilizes the transverse beam profile.

This stabilization effect can be understood qualitatively by considering that the diffusion process is an efficient decay process for small structures, but relatively inefficient for larger structures. As a result, the optical pumping process induces a waveguide that is smoother than it would be in the absence of atomic motion, thereby preventing the beam from breaking apart. In addition, the width of the waveguide can be larger than the width of the laser beam, resulting in better confinement of the beam. The existence of these stable solutions is not a contradiction of Derrick's theorem [6], although these two-dimensional structures are stable against the scaling perturbations considered by Derrick. Not only are the solutions time dependent, but the conditions considered here do not agree with the assumptions used by Derrick: for the proof of his theorem, Derrick assumed that the refractive index depends only on the local intensity.

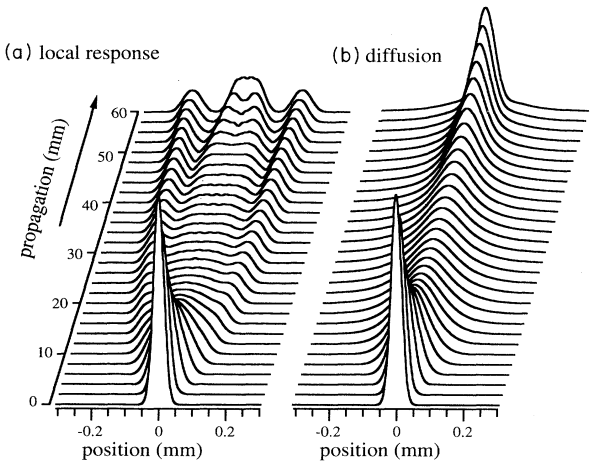


FIG. 2. Propagation of a laser beam in a medium with local response (a) and an atomic vapor with diffusive atomic motion (b). The absolute value of the laser-beam amplitude is plotted as a function of the distance from the center of the laser beam as it propagates into the medium.

For the calculation presented here, we have chosen $\Delta n > 0$, corresponding to blue detuning. Since $\Delta n$ changes sign when the laser is tuned through resonance, we expect self-defocusing for red detuning; this has indeed been found in an analogous calculation. While the calculations presented here assumed an ideal lossless atomic medium, we expect, of course, additional effects, such as absorption losses, to influence the process in the real medium.

For an experimental observation of these effects, we used a setup that is shown schematically in Fig. 3. The atomic medium, sodium vapor in our system, was contained in a heated cylindrical glass cell with a diameter of 25 mm and a length of 40 mm. To obtain a homogeneous optical resonance line, and to reduce the diffusion rate, 150 mbar of argon was added as a buffer gas; the collisional broadening caused a homogeneous linewidth of 1.7 GHz, somewhat larger than the Doppler width. Three orthogonal pairs of Helmholtz coils were used to cancel the Earth's magnetic field and to generate an adjustable magnetic field as a control for the loss mechanisms that counteract the optical pumping process. The magnetic field therefore provides the possibility to adjust the laser intensity at which the optical nonlinearity saturates, and simultaneously the distance over which diffusion is effective. The laser beam was derived from a single-mode cw ring dye laser (short-term linewidth $<500$ kHz) whose frequency was tuned close to the Na $D_1$ line ($\lambda=589.6$ nm). The laser beam was circularly polarized, and it was focused on the entrance window of the Na cell (beam waist $=33$ $\mu$m FWHM). The exit window of the Na cell was imaged onto a linear photodiode array, thereby enlarging the linear dimensions by a factor of 4. The dark-shaded area in Fig. 3 corresponds to the path of the self-focused beam, while the light-shaded area shows the propagation of the beam in a linear medium. The detector output was digitized and transferred to a computer for data storage and analysis.

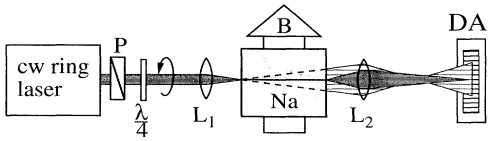


FIG. 3. Schematic representation of the experimental setup. $P$=polarizer, $\lambda/4$=retardation plate, $B$=adjustable magnetic field, $L_{1,2}$=lenses: $L_1$ focuses the incident beam onto the entrance window of the Na cell, while $L_2$ images the exit window onto the photodiode array DA. The dark-shaded region shows the beam path with self-trapping; the light-shaded and dashed area corresponds to the free beam.

Instead of measuring the beam profile as a function of the cell length, as in the theoretical results of Fig. 2, we measured the beam profile behind a cell of constant dimensions, but increased the effective optical path length by raising the cell temperature and thereby the particle density. In this way, the onset of self-focusing could easily be observed, as shown in Fig. 4, where the observed beam profile is plotted for different cell temperatures: the curves in Fig. 4(a) show the observed beam profiles at three different temperatures, while the data of Fig. 4(b) represent the measured beamwidths (FWHM) over a range of temperatures. For these measurements, the laser frequency was kept constant, at $\Delta = 10$ GHz above the resonance frequency, and the external magnetic field was set to zero. A 45-mW laser beam was focused onto the entrance window, resulting in an intensity of 7 kW cm$^{-2}$, an order of magnitude above the observed critical intensity. The beam diameters were determined from the digitized data and the geometrical enlargement by the imaging system was taken into account to calculate the beam diameter at the exit window that is plotted in the figure. The data clearly show the decrease of the beam diameter for increasing temperature, demonstrating the increasing importance of self-focusing as the refractive-index change increases. Above 205 °C, a further temperature increase does not cause an additional decrease of the beam diameter, indicating saturation of the self-focusing process and a stable, self-trapped beam. The shallow minimum at 205 °C may indicate a soliton oscillation.

In order to verify that the observed effect is indeed due to optical-pumping-induced changes of the refractive index, we measured the laser frequency dependence of the beam diameter at the exit window. The results are summarized in Fig. 5, where the measured beam profile at the exit window of the Na cell is shown for different laser frequencies. The squares indicate the width of the laser beam (FWHM) while the insets show full beam profiles at three representative wavelengths. The dotted vertical line indicates the position of the absorption maximum. As discussed above, the effect of the optical pumping process on the index of refraction is to bring it closer to 1. Because the index of refraction of a thin resonant medium is smaller than 1 for blue-detuned light, and larger than 1 on the red-detuned side, optical pumping induces a positive $\Delta n$ at shorter wavelengths and a negative $\Delta n$ for longer wavelengths. We therefore expect the laser beam to self-focus on the blue side and self-defocus on the red side. Obviously, the experimental data are in good agreement with this qualitative argument: the beam becomes self-trapped on the blue side of the resonance, while it self-defocuses when the laser is detuned to the red. The horizontal dashed line indicates the limit that is reached far off resonance. This frequency dependence shows clearly that dispersive effects are the cause of the reduced beam diameter. The same overall behavior was also observed with direct optical saturation [5]. Absorptive effects, which can also contribute [26–29], may become important near the center of the resonance line; they may be responsible for the fact that on resonance, where intensity-dependent changes of the refractive index should vanish, the beamwidth still appears to be narrower than far from resonance.

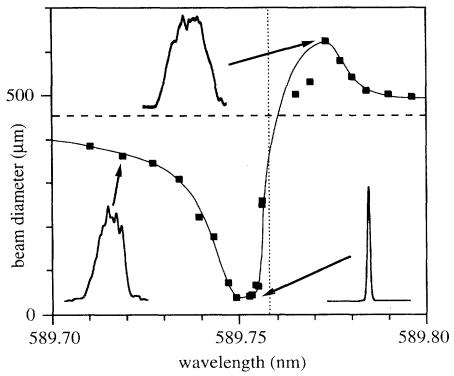


FIG. 5. Beam diameter (FWHM) of the laser beam at the exit window as a function of the laser wavelength (black squares). The insets show three different beam profiles for the wavelengths indicated by the arrows. The line through the squares is intended as a guide to the eye and does not represent a theoretical curve.

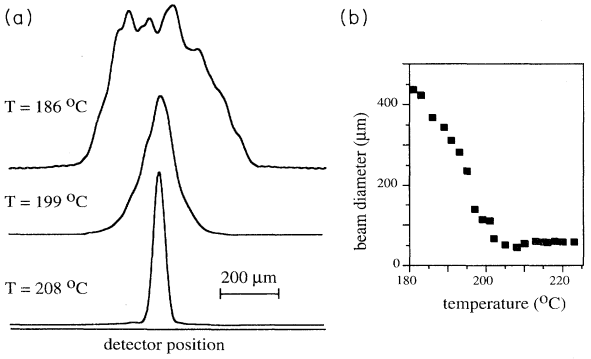


FIG. 4. (a) Beam profiles for three different temperatures corresponding to different (nonlinear) optical path lengths; the laser is blue detuned from the Na $D_1$ transition ($\Delta = 10$ GHz). (b) Beam diameter (FWHM) at the exit window as a function of temperature.

The results presented here were obtained with a small longitudinal magnetic field to stabilize the optical-pumping-induced magnetization in the sodium atoms. Applying transverse fields instead caused a significant decrease of the transmitted light intensity, a clear indication that the effect is induced by optical pumping. Apart from the intensity, transverse magnetic fields also affected the shape of the transmitted laser beam, an effect that was especially striking when the beam was no longer trapped, but split up into partial beams or formed ring structures. These observations are in qualitative agreement with theoretical predictions of magnetic-field-induced beam displacements [30].

The self-trapping of light in resonant media is, of course, limited by absorption losses that were not explicitly considered here. Due to the different dependence of absorption losses (quadratic) and dispersive effects (linear) on the optical detuning, these losses can be reduced by increasing the laser detuning. Within our scheme, they

cannot be eliminated completely, since they are part of the optical pumping process that generates the nonlinearity; however, the beam traveling inside the self-induced waveguide experiences a considerably reduced absorption, compared to the case of linear propagation. More sophisticated methods to reduce absorption, while keeping dispersive effects high, are also known [31,32] and may be applicable to self-trapped beams.

The experimental results reported here were measured under conditions where a single, stable beam was observed behind the interaction region. However, during our experiments, we also found parameter ranges where the beam profile appeared to be unstable. We observed ring structures, splitting of the beam into two partial beams, as well as more complicated structures. These instabilities resemble closely the kaleidoscopic spatial instabilities which Grantham *et al.* observed by introducing aberrations into the beam [33]. They indicate that the stabilization of the self-trapped beam by the saturation process and the nonlinear response of the medium is effective only in a limited parameter range. Within this parameter range, however, self-trapped beams cannot only propagate with an invariant cross section, but it is even possible that beams with different polarizations bounce off each other [34].

In conclusion, we have presented theoretical and experimental results demonstrating the generation of transverse solitary waves in the form of stable, self-trapped laser beams in a three-dimensional medium. The nonlinear response of the medium was induced by optical pumping, which requires only very small laser intensity. The nonlinearity saturates when the medium is fully polarized, thereby preventing the beam from collapsing. In addition, we have identified the nonlocal response of the medium due to the atomic motion as an important factor that stabilizes the beam profile. A relatively simple model appears to give a qualitatively correct description of the experimentally observed results.

We would like to thank Professor Raymond Chiao for helpful discussions. This work was supported by the Schweizerischer Nationalfonds.

[1] G. A. Askar'yan, Zh. Eksp. Teor. Fiz. **42**, 1567 (1962) [Sov. Phys. JETP **15**, 1088 (1962)].
[2] M. Hercher, J. Opt. Soc. Am. **54**, 563 (1964).
[3] Y. R. Shen, *The Principles of Nonlinear Optics* (Wiley, New York, 1984).
[4] R. Y. Chiao, E. Garmire, and C. H. Townes, Phys. Rev. Lett. **13**, 479 (1964).
[5] J. E. Bjorkholm and A. Ashkin, Phys. Rev. Lett. **32**, 129 (1974).
[6] G. H. Derrick, J. Math. Phys. **5**, 1252 (1964).
[7] J. H. Marburger and E. Dawes, Phys. Rev. Lett. **21**, 556 (1968).
[8] S. Maneuf, R. Desailly, and C. Froehly, Opt. Commun. **65**, 193 (1988).
[9] S. Maneuf and F. Reynaud, Opt. Commun. **66**, 325 (1988).
[10] J. S. Aitchison, A. M. Weiner, Y. Silberberg, M. K. Oliver, J. L. Jackel, D. E. Leaird, E. M. Vogel, and P. W. E. Smith, Opt. Lett. **15**, 471 (1990).
[11] A. W. Snyder, D. J. Mitchell, L. Poladian, and F. Ladouceur, Opt. Lett. **16**, 21 (1991).
[12] M. Karlsson, Phys. Rev. A **46**, 2726 (1992).
[13] T. K. Gustafson, P. L. Kelley, R. Y. Chiao, and R. G. Brewer, Appl. Phys. Lett. **12**, 165 (1968).
[14] D. Grischkowsky, Phys. Rev. Lett. **24**, 866 (1970).
[15] W. G. Wagner, H. A. Haus, and J. H. Marburger, Phys. Rev. **175**, 256 (1968).
[16] M. G. Boshier and W. J. Sandle, Opt. Commun. **42**, 371 (1982).
[17] M. LeBerre, E. Ressayre, and A. Tallet, J. Opt. Soc. Am. B **2**, 956 (1985).
[18] A. W. McCord, R. J. Ballagh, and J. Cooper, J. Opt. Soc. Am. B **5**, 1323 (1988).
[19] T. Yabuzaki, H. Hori, and M. Kitano, Jpn. J. Appl. Phys. **21**, 504 (1982).
[20] F. Mitschke, R. Deserno, W. Lange, and J. Mlynek, Phys. Rev. A **33**, 3219 (1986).
[21] D. Suter and J. Mlynek, in *Advances in Magnetic & Optical Resonance,* edited by W. S. Warren (Academic, San Diego, 1991), Vol. 16, pp. 1–63.
[22] D. Suter, Phys. Rev. A **46**, 344 (1992).
[23] M. Tanaka, T. Ohshima, K. Katori, M. Fujiwara, T. Itahashi, H. Ogata, and M. Kondo, Phys. Rev. A **41**, 1496 (1990).
[24] H. G. Dehmelt, Phys. Rev. **105**, 1487 (1957).
[25] W. Lange, G. Ankerhold, M. Schiffer, D. Mutschall, and T. Scholz (unpublished).
[26] M. LeBerre, E. Ressayre, and A. Tallet, Phys. Rev. A **25**, 1604 (1982).
[27] M. LeBerre, E. Ressayre, and A. Tallet, Phys. Rev. A **29**, 2669 (1984).
[28] M. LeBerre, E. Ressayre, A. Tallet, K. Tai, H. M. Gibbs, M. C. Rushford, and N. Peyghambarian, J. Opt. Soc. Am. B **1**, 591 (1984).
[29] D. E. McClelland, R. J. Ballagh, and W. J. Sandle, J. Opt. Soc. Am. B **3**, 212 (1986).
[30] R. J. Ballagh and A. W. McCord (unpublished).
[31] M. Fleischhauer, C. H. Keitel, M. O. Scully, C. Su, B. T. Ulrich, and S. Y. Zhu, Phys. Rev. A **46**, 1468 (1992).
[32] U. Rathe, M. Fleischhauer, S. Y. Zhu, T. W. Haensch, and M. O. Scully, Phys. Rev. A **47**, 4994 (1993).
[33] J. W. Grantham, H. M. Gibbs, G. Khitrova, J. F. Valley, and X. Jiajin, Phys. Rev. Lett. **66**, 1422 (1991).
[34] R. Holzner, P. Eschle, A. W. McCord, and D. M. Warrington, Phys. Rev. Lett. **69**, 2192 (1992).

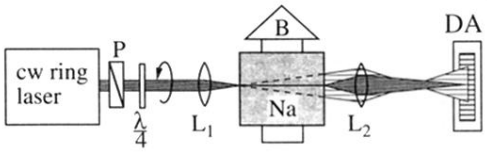


FIG. 3. Schematic representation of the experimental setup. $P$=polarizer, $\lambda/4$=retardation plate, $B$=adjustable magnetic field, $L_{1,2}$=lenses: $L_1$ focuses the incident beam onto the entrance window of the Na cell, while $L_2$ images the exit window onto the photodiode array DA. The dark-shaded region shows the beam path with self-trapping; the light-shaded and dashed area corresponds to the free beam.